RNA Modification

International Edition: DOI: 10.1002/anie.201810946
German Edition: DOI: 10.1002/ange.201810946

AlkAniline-Seq: Profiling of m^7G and m^3C RNA Modifications at Single Nucleotide Resolution

*Virginie Marchand, Lilia Ayadi, Felix G. M. Ernst, Jasmin Hertler, Valérie Bourguignon-Igel, Adeline Galvanin, Annika Kotter, Mark Helm, Denis L. J. Lafontaine, and Yuri Motorin**

Abstract: *RNA modifications play essential roles in gene expression regulation. Only seven out of >150 known RNA modifications are detectable transcriptome-wide by deep sequencing. Here we describe a new principle of RNAseq library preparation, which relies on a chemistry based positive enrichment of reads in the resulting libraries, and therefore leads to unprecedented signal-to-noise ratios. The proposed approach eschews conventional RNA sequencing chemistry and rather exploits the generation of abasic sites and subsequent aniline cleavage. The newly generated 5′-phosphates are used as unique entry for ligation of an adapter in library preparation. This positive selection, embodied in the AlkAniline-Seq, enables a deep sequencing-based technology for the simultaneous detection of 7-methylguanosine (m^7G) and 3-methylcytidine (m^3C) in RNA at single nucleotide resolution. As a proof-of-concept, we used AlkAniline-Seq to comprehensively validate known m^7G and m^3C sites in bacterial, yeast, and human cytoplasmic and mitochondrial tRNAs and rRNAs, as well as for identifying previously unmapped positions.*

RNA modifications are playing essential roles in gene expression regulation.[1–3] Only seven (m^6A, m^6Am, m^1A, m^5C, hm^5C, Nm and ψ) out of >150 RNA modifications are detectable transcriptome-wide by deep sequencing.[4–10] Modified nucleotides in tRNA, rRNA and mRNA do not only affect RNA processing, transport and stability, but these residues also impact mRNA translation.[11–15] Despite these important findings, details are scarce and disputed on the distribution and functions of many modified nucleotides in different transcriptomes. Only recently, high-throughput sequencing (NGS) methods coupled to antibody-directed enrichment provided comprehensive maps of m^6A and m^1A residues in different species.[16–18] For other RNA modifications, the use of specific chemical reagents allowed their high-throughput mapping.[7,19–22] While these approaches brought important discoveries in the field, several challenges remain open. For once, the list of NGS-detectable RNA modifications is still extremely restricted. Considering that the natural RNA modification repertoire comprises >150 modifications, there is an urgent need to develop novel chemistry of detection, ideally directly amenable to deep sequencing.

Here we report a fundamentally new detection principle that hinges upon a chemistry-based enrichment of RNAseq library with RNA fragments containing certain modifications. The first clues in the discovery of this highly effective method emerged from the application of traditional chemical treatments to induce cleavage in RNAs containing m^7G, for which this specific detection in RNA was described in the 70's.[23,24] We initially intended to apply sequential treatments with sodium borohydride ($NaBH_4$) and aniline, for high throughput detection of cleavage sites. We found that $NaBH_4$ reduction combined with subsequent aniline cleavage of the resulting abasic site[25] produced high background, as is typical for detection of abortive cDNA.[26] Coupling to deep sequencing, this technique produced signals at some known m^7G sites in tRNAs and rRNA, but also led to numerous false discovery hits (Figure S1 in the Supporting Information) thus making it unsuitable for a search of m^7G in low abundant RNAs.

We therefore reasoned, that the 5′-phosphate generated during the aniline cleavage could be exploited as a selective entry into a library preparation including a limiting ligation step with exactly such phosphate as prerequisite (Figure 1b and Figure S2a). This approach did not only yield very clear signals, but, in addition, revealed that the $NaBH_4$treatment could be omitted in favor of a limited alkaline hydrolysis. The resulting novel approach (named AlkAniline-Seq) can map abasic sites and modified nucleotides that generate the latter upon treatment. AlkAniline-Seq combines three successive treatments: i) RNA alkaline hydrolysis, ii) extensive 5′- and 3′-dephosphorylation and iii) aniline cleavage (Figure 1a). According to the literature,[27,28] m^7G residues are subject of nucleophilic attack by hydroxide anions, a reaction that ultimately leads to ring opening, base elimination and creation of an abasic site.[29]

Upon exposing m^7G nucleosides to the alkaline conditions of the AlkAniline-Seq protocol, known intermediates of this

[*] V. Marchand, L. Ayadi, V. Bourguignon-Igel, Y. Motorin
Lorraine University, UMS2008 IBSLor CNRS-UL-INSERM, Biopôle UL
9, Avenue de la Forêt de Haye, 54505 Vandoeuvre-les-Nancy (France)
E-mail: Yuri.Motorin@univ-lorraine.fr
L. Ayadi, V. Bourguignon-Igel, A. Galvanin, Y. Motorin
Lorraine University, UMR7365 IMoPA CNRS-UL, Biopôle UL
9, Avenue de la Forêt de Haye, 54505 Vandoeuvre-les-Nancy (France)
F. G. M. Ernst, D. L. J. Lafontaine
RNA Molecular Biology, ULB-Cancer Research Center (U-CRC), Center for Microscopy and Molecular Imaging (CMMI), Fonds National de la Recherche (F.R.S./FNRS) and Université Libre de Bruxelles (ULB), BioPark campus Gosselies (Belgium)
J. Hertler, A. Kotter, M. Helm
Institute of Pharmacy and Biochemistry
Johannes Gutenberg University Mainz
Staudingerweg 5, 55128 Mainz (Germany)

Supporting information (methods, including statements of data availability and any associated accession codes and references) and the ORCID identification number(s) for the author(s) of this article can be found under https://doi.org/10.1002/anie.201810946. The datasets generated and analyzed in the current study are available in the European Nucleotide Archive, accession number PRJEB26005.

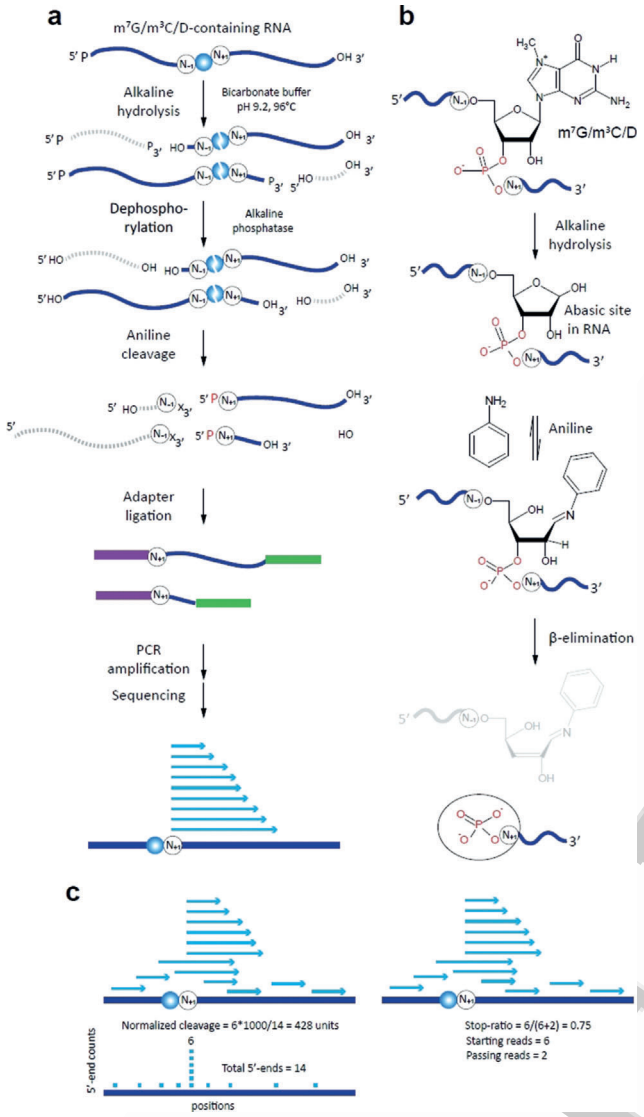

Figure 1. Overview of the AlkAniline-Seq technology. a) Schematic representation of the RNA chain cleavage and primer ligation to unique 5′-phosphates resulting from abasic site decomposition. Enrichment of sequencing reads starting at the nucleotide $N+1$ is shown. Modified residue (m^7G, m^3C or D) is shown as a blue dot. Broken blue dot corresponds to RNA abasic site. b) Chemical reactions leading to the formation of an abasic site at $m^7G/m^3C/D$ residues in RNA. The first step consists of an alkaline hydrolysis (RNA fragmentation), and the second step is an aniline cleavage followed by β-elimination of ribose-aniline adduct. c) Principles of scoring of AlkAniline-Seq signals by counting of 5′-reads' extremities and calculation of normalized cleavage (left) or Stop-ratio (right). Normalized cleavage is expressed in units (reads starting at a given position in RNA×1000/total number of reads aligned to this RNA, ranging from 5–25 units for background to a maximum of 1000 units for a single positive hit in RNA). "Stop-ratio" is calculated as the proportion of reads starting at a position out of all the reads overlapping it. "Stop-ratio" was extensively used so far in transcriptome-wide mapping of RNA modifications (e.g. in Ψ-seq[12]).

decay pathway were indeed detected by LC-MS (Figure S2bcd), which is consistent with the subsequent formation of abasic sites.[25] The second step of the AlkAniline-Seq protocol consists in RNA fragment end-repaired by extensive treatment with alkaline phosphatase to remove both pre-existing 5′-phosphates in RNA and all forms of 3′-phosphates resulting from alkaline hydrolysis (Figure 1a).

Subsequently, all obtained RNA fragments are expected to have 5′- and 3′- OH extremities, compatible with 3′-ligation, but still precluding 5′-adapter ligation; this latter step strictly requires the pivotal 5′-phosphate.

The aniline treatment of the third step then leads to cleavage at abasic sites by subsequent β- and δ-elimination (Figure 1b), resulting effectively in the deprotection of the 5′-phosphate at the $N+1$ nucleotide.[25] Thus, these 5′-phosphate-containing RNA fragments are only released after aniline treatment and exclusively from modified nucleosides such as m^7G (Figure 1b). A positive enrichment of the aniline cleaved fragments is functionally implemented in this selective ligation protocol, ultimately forming the basis for the high sensitivity and specificity of this approach. Unlike conventional RNAseq approaches, AlkAniline-Seq provides a qualified pool of reads, where the information about modified sites resides at the 5′-extremity of each read. The dsDNA amplicons resulting from library preparation were sequenced using Illumina technology, where the beginning of Read1 corresponds to the $N+1$ nucleotide deprotected by decomposition of abasic site. Hence, the reads were mapped to the reference sequence in end-to-end mode, and count of reads' 5′-extremities indicated the position and intensity of the cleavage.

Detection of m^7G residues was first conducted in *S. cerevisiae* 18S rRNA which contains a unique m^7G1575, formed by the 18S rRNA:m^7G1575-methyltransferase complex Bud23/Trm112[30,31] (Figure 2a). Yeast strains and sequencing libraries used in the study are described in Tables S1 and S2.

As shown in Figure 2b, AlkAniline-Seq produced a single hit with a cleavage score of ≈400 units in WT 18S rRNA precisely at the position of m^7G1575. This signal was absent either when aniline treatment was omitted, or when RNA from a *bud23Δ* yeast strain was used for analysis (Figure 2b). LC-MS measurements confirmed that WT 18S rRNA contained 1.04 ± 0.05 m^7G, while only a background value was detected in *bud23Δ* strain (Figure 2b inset). No signals were detected in yeast 25S rRNA, confirming the high specificity of the method for m^7G detection (Figure S3a). Furthermore, biological and technical replicates show a robust and consistent signal for m^7G1575 (Figure S3b). As further validation, two known m^7G sites in *E. coli* rRNA (m^7G527 in 16S rRNA and m^7G2069 in 23S rRNA)[32] were detected by two strong signals at the expected positions (Figure S5ab).

Both alkaline hydrolysis at high pH and extensive 5′-dephosphorylation of RNA fragments before aniline cleavage were essential for high specificity. Replacement of alkaline hydrolysis at high pH with equivalent Mg^{2+} fragmentation did not yield any signal in either 18S or 25S rRNA (Figure S3cd) and when the 5′/3′-dephosphorylation was limited to 3′-dephosphorylation only by using T4 PNK (Figure S4a), the signal for m^7G dropped dramatically to only ≈20 units (Figure S4b).

The sensitivity of m^7G detection was evaluated using calibration mixtures composed of total RNA from WT and

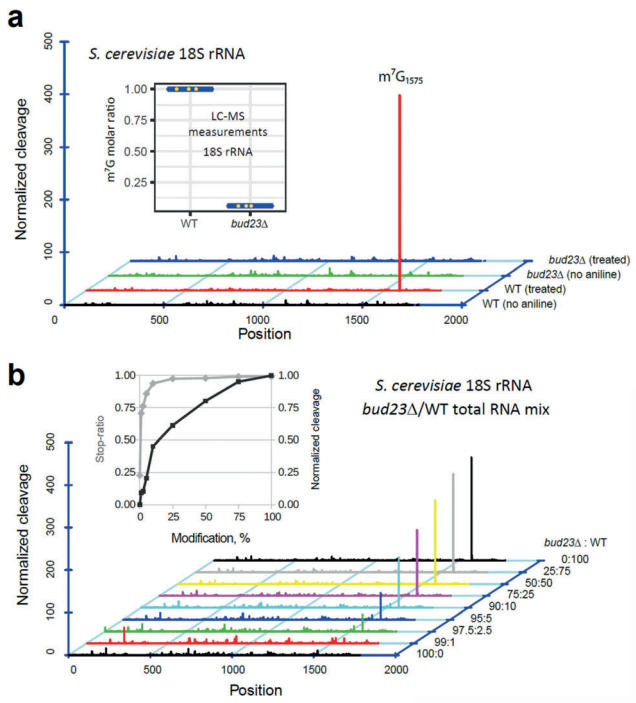

Figure 2. Detection and quantification of the unique m^{7}G1575 residue in *S. cerevisiae* 18S rRNA. a) Influence of aniline treatment on the level of observed m^{7}G1575 signal. Normalized cleavage at m^{7}G1575 in WT and *bud23Δ* 18S rRNA in mock experiment (no aniline) and in aniline-treated samples (treated) by RNA position. The m^{7}G1575 is only detected in the wild-type treated sample. The inset gives LC-MS quantification of m^{7}G molar amount in WT and *bud23Δ* 18S rRNA. Molar amount is a mean of $n=3$ independent measurements, which are shown as yellow dots (b) Sensitivity of m^{7}G detection in mixes of unmodified (*bud23Δ*) and modified (WT) 18S rRNA. Proportion of modified 18S rRNA varied from 0 to 100% (indicated to the right). Inset gives a trace of normalized cleavage (in black) and Stop-ratio (in grey) as a function of molar ratio of m^{7}G1575 modification.

bud23Δ (KO strain for m^{7}G1575), with the proportion of m^{7}G1575-containing WT rRNA varying from 1 to 100%. Remarkably, a saturation curve of the signal was obtained (Figure 2c), where the signal is well visible over background

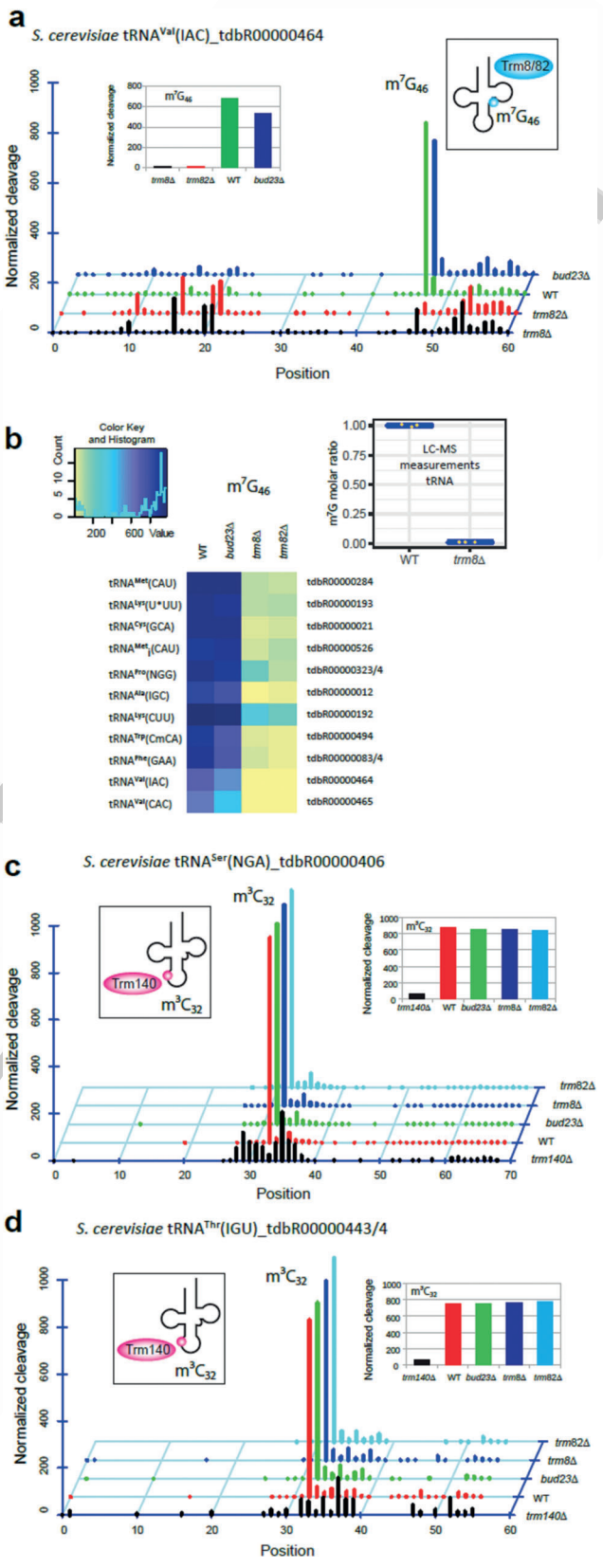

Figure 3. Detection of m^{7}G46 and m^{3}C32 residues in *S. cerevisiae* tRNAs. a) Normalized cleavage signals for *S. cerevisiae* tRNA^{Val}(IAC) in *trm8Δ*, *trm82Δ*, WT and *bud23Δ* yeast strains. Inset on the right shows the cloverleaf structure of tRNA with the modified position and the corresponding enzymatic activity (heterocomplex Trm8/Trm82). Inset on the left gives quantification of normalized cleavage in the four strains used. b) Heat map shows normalized cleavage values for all *S. cerevisiae* RNAs containing m^{7}G residues in the same strains. LC-MS quantification of the residual m^{7}G content in tRNA fraction from *trm8Δ* strain is also shown. Molar amount is a mean of n = 3 independent measurements shown on the Figure as yellow dots. The residual signals for tRNA^{Pro}(NGG) and tRNA^{Lys}(CUU) in *trm8Δ* and *trm82Δ* strains, are not due to residual m^{7}G level, but correspond to incomplete dephosphorylation of some positions in the compact 3D tRNA structure. c,d) Normalized cleavage signals for *S. cerevisiae* tRNA^{Ser}(NGA) and tRNA^{Thr}(IGU) in *trm140Δ*, WT, *bud23Δ*, *trm8Δ* and *trm82Δ* yeast strains. Inset on the left shows the cloverleaf structure of tRNA with the modified position and corresponding enzymatic activity (Trm140). Inset on the right gives quantification of normalized cleavage in the different strains used.

Dateiname: Z810946e
Pfad: l:/daten/verlage/vch/ach/hefte/pool/
Status Neusatz
Datum: 45 KW., 6. November 2018 (Dienstag)
Pagina: 3
Seite: 3 te von 8
Umfang (Seiten): 8
Zeit: 10:41:35 Uhr

value already at ≈2% of modified RNA, which is unprecedented in any RNAseq approach for RNA detection. This demonstrates a high sensitivity of AlkAniline-Seq even for the detection of substoichiometrically modified m^7G sites.

A first application consisted in the faithful mapping of all 10 previously known m^7G sites in yeast tRNAs, all of which depend on the Trm8/Trm82 complex[33] (Figure 3a and Figure S6a). A heat map summarizing normalized cleavage efficiency for yeast m^7G-containing tRNAs[34] for WT, *bud23Δ*, *trm8Δ* and *trm82Δ* strains is shown in Figure 3b. In addition to known sites, a readily detectable signal for m^7G46 residue was detected in $tRNA^{Ala}$(IGC) in WT and *bud23Δ* cells, but not in *trm8Δ*/*trm82Δ* strains, thus identifying a new substrate of the Trm8/Trm82 complex (Figure 3b and Figure S7). A further application to *E. coli* tRNAs successfully detected all known m^7G positions, without any false-positive hits (representative examples are shown in Figure S5c).

An inspection of the above results at residues other than guanosines identified further strong signals at selected cytosines and uridines, strongly suggesting that the specificity of AlkAniline-Seq, was not limited to m^7G, but reacted to additional of the altogether 46[34] modifications present in yeast and *E. coli.* In particular, the AlkAniline-Seq profiles for yeast $tRNA^{Ser}$ and $tRNA^{Thr}$ showed a consistent and prominent signal in the anticodon loop, which corresponds to m^3C32 (known to be modified by Trm140).[35]

Accordingly, in both tRNAs, the signal specifically disappeared in *trm140Δ* yeast strain (Figure 3c,d, Figure S6c). However, exposure of m^3C nucleoside to alkaline conditions showed only deamination to m^3U (Figure S8), which is not reactive in AlkAniline-Seq.

Dihydrouridine (D) in yeast and bacterial tRNAs also provided detectable signal in AlkAniline-Seq. Signals were observed for a limited subset of known D residues in tRNAs and the relative signal strength was comparably lower (100–300 units) (Figure S9). To validate consistency of D detection, we performed AlkAniline-Seq analysis on yeast mutants carrying a deletion of one of the four known tRNA:dihydrouridine synthases (Dus1, Dus2, Dus3, and Dus4), responsible for formation of D16/D17, D20, D47 and D20ab, respectively.[36,37] Analysis of D signals for tRNAs and their absence in respective knockout strains followed previous assignments of DUS genes to D sites in tRNAs. Thus, AlkAniline-Seq responds to the presence of D, although the signal strength is considerably lower than for m^7G and m^3C, likely due to incomplete formation of abasic sites from D. While the chemistry of m^7G detection could be readily reenacted (Figure S2), deeper investigations must clarify the basis for the detection of m^3C and D.

AlkAniline-Seq was further applied to human cytoplasmic and mitochondrial rRNAs and tRNAs. Using total RNA as a starting material, we established a complete profile of m^7G, m^3C and D sites in these RNA molecules (Table S3). As anticipated, analysis of rRNAs revealed a single 18S-m^7G1639 residue,[38] without additional signals in other human cytoplasmic and mitochondrial rRNA species (Figure S10). Profiling of human cytoplasmic and mitochondrial tRNAs revealed seventeen m^7G, twelve m^3C and thirty-three D sites (Figure 4, Table S4). This comprehensive listing once more

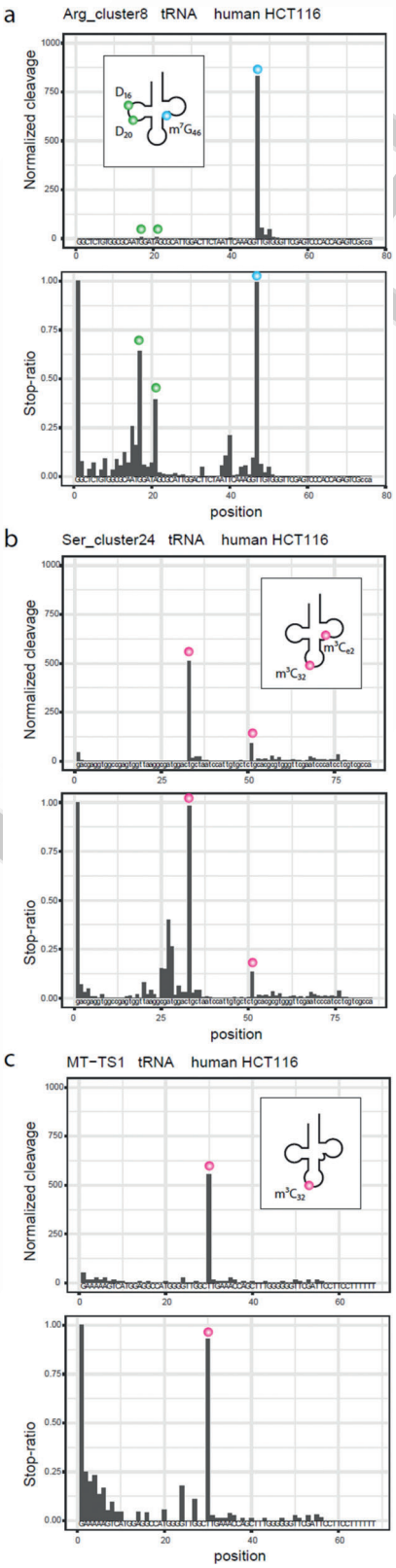

Figure 4. Detection of m^7G, m^3C and D residues in *Homo sapiens* cytoplasmic and mitochondrial tRNAs. a) Normalized cleavage (top panels) and Stop-ratio (bottom panels) profiles for selection of human tRNAs ($tRNA^{Arg}$(TCT), b) $tRNA^{Ser}$(GCT) and c) mitochondrial $tRNA^{Ser1}$-(TCA). Insets show the cloverleaf structure of tRNA with the modified residues indicated by colored spheres. Position e2 in the variable loop of human $tRNA^{Ser}$(GCT) was previously found to be modified to m^3C.

illustrates the exceptional sensitivity of the method, given that some of the low-abundant RNA species were only present in pg amounts.

The presence of m^7G, m^3C and D in eukaryotic mRNA is still questionable, even if some of these nucleotides were reported.[39] To perform our analysis transcriptome-wide, yeast poly(A)-enriched mRNA fraction was subjected to AlkAniline-Seq, converted to library and sequenced. The resulting reads were aligned to the yeast SacCer3 genome as well as to the RefSeq mRNA database. Stop-ratios between reads terminating at a given position and reads overlapping the same were calculated (Figure 1c).

Sufficient amount of sequencing information (>100 reads coverage per mRNA) was obtained for ≈ 1500 yeast mRNAs. However, only very few (<20) hits satisfied the criteria validated for rRNA and tRNA (Stop-ratio >0.75 and >100 reads coverage). The majority of them were either cryptic tRNA sequences or transcription start sites of highly expressed yeast genes, most probably due to incomplete dephosphorylation of m^7G-capped mRNAs during step 2 of the protocol (Figure S11). Moreover, no $m^7G/m^3C/(D)$ signals were detected for non-polyadenylated yeast ncRNA (snRNAs, snoRNAs, etc).

In conclusion, AlkAniline-Seq illustrates a new concept for the high-throughput detection of modified RNA nucleotides by deep sequencing: a specific sequence of chemical reactions leading to the production of RNA fragments cleaved at the $N+1$ nucleotide to the modification site, and those fragments are selectively converted into sequencing libraries. This dramatically increases the specificity and the sensitivity of the approach, since the only other sources of accessible 5′-phosphate residues are seldom.

Another interesting property of AlkAniline-Seq is that it simultaneously detects at least two different RNA modifications, namely: m^7G and m^3C, and, at lower extent, D. Since these modified nucleotides are derived from different parental nucleotides they are readily distinguishable when the reads are aligned.

We foresee multiple applications for AlkAniline-Seq $m^7G/m^3C/(D)$ mapping in organisms where RNA modification has not been systematically addressed, which includes many model organisms in developmental biology. Further perspectives include putative stress-inducible and disease-specific modifications in mRNA and ncRNAs other than tRNA/rRNAs in various biological and pathological contexts.[40,41] AlkAniline-Seq could also be used for profiling of 16S-m^7G1405-dependent aminoglycoside resistance in gram-negative bacteria[42] and in other biomedical projects aimed at studying the dynamics and regulation of m^7G, m^3C, and D in diverse biological context.

Acknowledgements

Y.M. was supported by ANR-DFG grant HTRNA-Mod ANR-13-ISV8-0001 and Research funds from Lorraine Région (France). M.H. was supported by the DFG (HE3397/8-1, HE3397/13-2, SPP1784). The Lab of D.L.J.L. is supported by the Université Libre de Bruxelles (ULB), the Fonds National de la Recherche (F.R.S./FNRS), the Walloon Region (DGO6), and the Fédération Wallonie-Bruxelles. Work performed in the frame of the COST EPITRAN network.

Conflict of interest

The authors declare no conflict of interest.

Keywords: abasic site · deep sequencing · epitranscriptomics · methylation · RNA modification

[1] D. Dominissini, *Science* **2014**, *346*, 1192.
[2] B. S. Zhao, I. A. Roundtree, C. He, *Nat. Rev. Mol. Cell Biol.* **2017**, *18*, 31–42.
[3] Y. Saletore, K. Meyer, J. Korlach, I. D. Vilfan, S. Jaffrey, C. E. Mason, *Genome Biol.* **2012**, *13*, 175.
[4] D. Dominissini, S. Moshitch-Moshkovitz, M. Salmon-Divon, N. Amariglio, G. Rechavi, *Nat. Protoc.* **2013**, *8*, 176–189.
[5] D. Dominissini, S. Nachtergaele, S. Moshitch-Moshkovitz, E. Peer, N. Kol, M. S. Ben-Haim, Q. Dai, A. Di Segni, M. Salmon-Divon, W. C. Clark, et al., *Nature* **2016**, *530*, 441–446.
[6] T. M. Carlile, M. F. Rojas-Duran, B. Zinshteyn, H. Shin, K. M. Bartoli, W. V. Gilbert, *Nature* **2014**, *515*, 143–146.
[7] S. Schwartz, D. A. Bernstein, M. R. Mumbach, M. Jovanovic, R. H. Herbst, B. X. León-Ricardo, J. M. Engreitz, M. Guttman, R. Satija, E. S. Lander, et al., *Cell* **2014**, *159*, 148–162.
[8] J. E. Squires, H. R. Patel, M. Nousch, T. Sibbritt, D. T. Humphreys, B. J. Parker, C. M. Suter, T. Preiss, *Nucleic Acids Res.* **2012**, *40*, 5023–5033.
[9] B. Delatte, F. Wang, L. V. Ngoc, E. Collignon, E. Bonvin, R. Deplus, E. Calonne, B. Hassabi, P. Putmans, S. Awe, et al., *Science* **2016**, *351*, 282–285.
[10] U. Birkedal, M. Christensen-Dalsgaard, N. Krogh, R. Sabarinathan, J. Gorodkin, H. Nielsen, *Angew. Chem. Int. Ed.* **2015**, *54*, 451–455; *Angew. Chem.* **2015**, *127*, 461–465.
[11] E. M. Harcourt, A. M. Kietrys, E. T. Kool, *Nature* **2017**, *541*, 339–346.
[12] P. J. Hsu, H. Shi, C. He, *Genome Biol.* **2017**, *18*, 197.
[13] A. Visvanathan, K. Somasundaram, *Bioessays* **2018**, https://doi.org/10.1002/bies.201700093.
[14] J. Choi, K.-W. Ieong, H. Demirci, J. Chen, A. Petrov, A. Prabhakar, S. E. O'Leary, D. Dominissini, G. Rechavi, S. M. Soltis, et al., *Nat. Struct. Mol. Biol.* **2016**, *23*, 110–115.
[15] J. Choi, G. Indrisiunaite, H. DeMirci, K.-W. Ieong, J. Wang, A. Petrov, A. Prabhakar, G. Rechavi, D. Dominissini, C. He, et al., *Nat. Struct. Mol. Biol.* **2018**, *25*, 208–216.
[16] X. Li, J. Peng, C. Yi, *Methods Mol. Biol.* **2017**, *1562*, 245–255.
[17] B. Molinie, J. Wang, K. S. Lim, R. Hillebrand, Z.-X. Lu, N. Van Wittenberghe, B. D. Howard, K. Daneshvar, A. C. Mullen, P. Dedon, et al., *Nat. Methods* **2016**, *13*, 692–698.
[18] M. Safra, A. Sas-Chen, R. Nir, R. Winkler, A. Nachshon, D. Bar-Yaacov, M. Erlacher, W. Rossmanith, N. Stern-Ginossar, S. Schwartz, *Nature* **2017**, *551*, 251–255.
[19] S. Hussain, J. Aleksic, S. Blanco, S. Dietmann, M. Frye, *Genome Biol.* **2013**, *14*, 215.
[20] M. Helm, Y. Motorin, *Nat. Rev. Genet.* **2017**, *18*, 275–291.
[21] S. Schwartz, Y. Motorin, *RNA Biol.* **2017**, *14*, 1124–1137.
[22] E. M. Novoa, C. E. Mason, J. S. Mattick, *Nat. Rev. Mol. Cell Biol.* **2017**, *18*, 339–340.

[23] V. S. Zueva, A. S. Mankin, A. A. Bogdanov, L. A. Baratova, *Eur. J. Biochem.* **1985**, *146*, 679 – 687.
[24] W. Wintermeyer, H. G. Zachau, *FEBS Lett.* **1975**, *58*, 306 – 309.
[25] P. A. Küpfer, C. J. Leumann, *Nucleic Acids Res.* **2007**, *35*, 58 – 68.
[26] R. Hauenschild, L. Tserovski, K. Schmid, K. Thüring, M.-L. Winz, S. Sharma, K.-D. Entian, L. Wacheul, D. L. J. Lafontaine, J. Anderson, et al., *Nucleic Acids Res.* **2015**, *43*, 9950 – 9964.
[27] C. J. Chetsanga, B. Bearie, C. Makaroff, *Chem.-Biol. Interact.* **1982**, *41*, 217 – 233.
[28] P. D. Lawley, P. Brookes, *Biochem. J.* **1963**, *89*, 127 – 138.
[29] C. J. Chetsanga, C. Makaroff, *Chem.-Biol. Interact.* **1982**, *41*, 235 – 249.
[30] J. White, Z. Li, R. Sardana, J. M. Bujnicki, E. M. Marcotte, A. W. Johnson, *Mol. Cell. Biol.* **2008**, *28*, 3151 – 3161.
[31] S. Figaro, L. Wacheul, S. Schillewaert, M. Graille, E. Huvelle, R. Mongeard, C. Zorbas, D. L. J. Lafontaine, V. Heurgué-Hamard, *Mol. Cell. Biol.* **2012**, *32*, 2254 – 2267.
[32] J. E. Smith, B. S. Cooperman, P. Mitchell, *Biochemistry* **1992**, *31*, 10825 – 10834.
[33] A. Alexandrov, M. R. Martzen, E. M. Phizicky, *RNA* **2002**, *8*, 1253 – 1266.
[34] P. Boccaletto, M. A. Machnicka, E. Purta, P. Piatkowski, B. Baginski, T. K. Wirecki, V. de Crécy-Lagard, R. Ross, P. A. Limbach, A. Kotter, et al., *Nucleic Acids Res.* **2018**, *46*, D303 – D307.
[35] S. D'Silva, S. J. Haider, E. M. Phizicky, *RNA* **2011**, *17*, 1100 – 1110.
[36] F. Xing, M. R. Martzen, E. M. Phizicky, *RNA* **2002**, *8*, 370 – 381.
[37] F. Xing, S. L. Hiley, T. R. Hughes, E. M. Phizicky, *J. Biol. Chem.* **2004**, *279*, 17850 – 17860.
[38] C. Zorbas, E. Nicolas, L. Wacheul, E. Huvelle, V. Heurgué-Hamard, D. L. J. Lafontaine, *Mol. Biol. Cell* **2015**, *26*, 2080 – 2095.
[39] J.-M. Chu, T.-T. Ye, C.-J. Ma, M.-D. Lan, T. Liu, B.-F. Yuan, Y.-Q. Feng, *ACS Chem. Biol.* **2018**, https://doi.org/10.1021/acschembio.7b00906.
[40] N. Jonkhout, J. Tran, M. A. Smith, N. Schonrock, J. S. Mattick, E. M. Novoa, *RNA* **2017**, *23*, 1754 – 1769.
[41] L. P. Sarin, S. A. Leidel, *RNA Biol.* **2014**, *11*, 1555 – 1567.
[42] N. Husain, K. L. Tkaczuk, S. R. Tulsidas, K. H. Kaminska, S. Čubrilo, G. Maravić-Vlahoviček, J. M. Bujnicki, J. Sivaraman, *Nucleic Acids Res.* **2010**, *38*, 4120 – 4132.

Manuscript received: September 26, 2018
Accepted manuscript online: October 29, 2018
Version of record online: ■■ ■■, ■■■■

Communications

RNA Modification

V. Marchand, L. Ayadi, F. G. M. Ernst, J. Hertler, V. Bourguignon-Igel, A. Galvanin, A. Kotter, M. Helm, D. L. J. Lafontaine, Y. Motorin* ——— ■■■■–■■■■

AlkAniline-Seq: Profiling of m^7G and m^3C RNA Modifications at Single Nucleotide Resolution

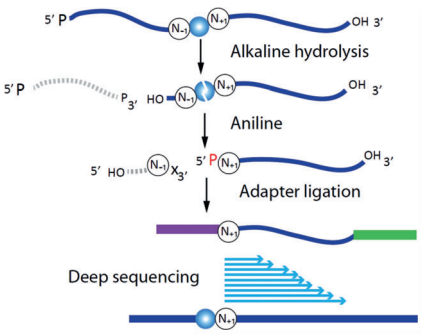

Deep sequencing was applied in a new concept of library preparation for detection of RNA modifications. Modified RNA is treated by alkaline hydrolysis, dephosphorylated and subjected to aniline cleavage of abasic sites. The resulting 5′-phosphates in RNA are used for specific ligation of the sequencing adapter. The method can be applied for specific and sensitive detection of m^7G, m^3C and (D) residues in RNAs.

RNA-Modifikationen

V. Marchand, L. Ayadi, F. G. M. Ernst, J. Hertler, V. Bourguignon-Igel, A. Galvanin, A. Kotter, M. Helm, D. L. J. Lafontaine, Y. Motorin* ——— ■■■■–■■■■

AlkAniline-Seq: Profiling of m^7G and m^3C RNA Modifications at Single Nucleotide Resolution

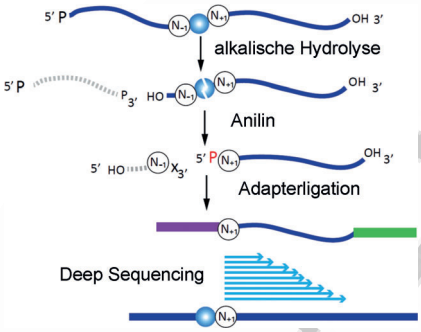

Deep Sequencing wurde genutzt, um ein neues Konzept für den Aufbau von Bibliotheken zum Nachweis spezifischer DNA-Modifikationen zu entwickeln. Modifizierte RNA wird alkalischer Hydrolyse ausgesetzt, dephosphoryliert und an abasischen Stellen mit Anilin gespalten. Die resultierenden 5′-Phosphate werden für die spezifische Ligation von Sequenzierungsadaptern genutzt. Die Methode kann für den spezifischen und empfindlichen Nachweis von m^7G, m^3C und (D)-Resten in RNAs verwendet werden.

SPACE RESERVED FOR IMAGE AND LINK

Share your work on social media! *Angewandte Chemie* has added Twitter as a means to promote your article. Twitter is an online microblogging service that enables its users to send and read short messages and media, known as tweets. Please check the pre-written tweet in the galley proofs for accuracy. If you, your team, or institution have a Twitter account, please include its handle @username. Please use hashtags only for the most important keywords, such as #catalysis, #nanoparticles, or #proteindesign. The ToC picture and a link to your article will be added automatically, so the **tweet text must not exceed 250 characters**. This tweet will be posted on the journal's Twitter account (follow us @angew_chem) upon publication of your article in its final (possibly unpaginated) form. We recommend you to re-tweet it to alert more researchers about your publication, or to point it out to your institution's social media team.

Please check that the ORCID identifiers listed below are correct. We encourage all authors to provide an ORCID identifier for each coauthor. ORCID is a registry that provides researchers with a unique digital identifier. Some funding agencies recommend or even require the inclusion of ORCID IDs in all published articles, and authors should consult their funding agency guidelines for details. Registration is easy and free; for further information, see http://orcid.org/.

Virginie Marchand
Lilia Ayadi
Felix G. M. Ernst
Jasmin Hertler
Valérie Bourguignon-Igel
Adeline Galvanin
Annika Kotter
Mark Helm
Denis L. J. Lafontaine
Yuri Motorin http://orcid.org/0000-0002-8018-334X

Author Contributions

V.M. and L.A. performed AlkAniline-Seq, F.E., A.G. and V.B.I. prepared strains/cell lines and extracted RNA, J.H. and A.K. performed LC-MS analysis, M.H., D.L.J.L. and Y.M. analysed the data and wrote the manuscript.

